

Oscillatory magnetic anisotropy tuned by interlayer coupling

D. H. Wei, X. Y. Xu, L. F. Yin, G. S. Dong, and X. F. Jin*

Surface Physics Laboratory, Fudan University, Shanghai 200433, China

(Received 8 May 2009; revised manuscript received 7 July 2009; published 10 September 2009)

The magnetic anisotropy and interlayer coupling of epitaxially grown Ni/Cu/Co sandwich on Cu(100) have been studied *in situ* as a function of Cu and Ni thicknesses by magneto-optic Kerr effect. Oscillatory magnetic anisotropy of Ni layer is observed and attributed to the oscillatory interlayer coupling between the Ni and Co layers.

DOI: [10.1103/PhysRevB.80.092403](https://doi.org/10.1103/PhysRevB.80.092403)

PACS number(s): 75.30.Et, 75.30.Gw

Magnetic anisotropy, which determines the “easy” and “hard” directions of magnetization, is one of the most important properties of magnetic materials. No matter what applications of the magnetic materials, proper magnetic anisotropy is always required. Furthermore the recently developed nonvolatile magnetic random access memory (MRAM),^{1,2} and related MRAM logic,³ rely on the proper control of the direction of magnetization in the nanoscale films or nanopatterns. The tailoring of the magnetic anisotropy is, indeed, important for these future applications.

Magnetic anisotropy can be affected by several factors, such as structure,⁴ film strain⁵ and thickness,⁶ broken symmetry at the surface/interface,^{7,8} and others, which provide the various options to tune the magnetic anisotropy. Interlayer coupling, the coupling between two magnetic layers sandwiched by nonmagnetic space layer, is also predicted to be one possible way to tune the magnetic anisotropy.⁹ It is well known that the interlayer coupling has an effect on magnetic properties such as magnetoresistance or Curie temperature (T_C). For example, the T_C of Ni layer in Ni/Cu/Co sandwich can be increased by 40 K through the interlayer coupling between the Ni and Co layers.¹⁰ However its effect on magnetic anisotropy is still not fully explored. Qiu and co-workers studied the Ni/Fe/Co (Ref. 11) and Fe/Cu/Ni (Ref. 12) sandwiches on Cu(100) by photoemission electron microscopy (PEEM) and observed that the critical thickness (d_c) of the Ni spin reorientation transition (SRT) in Ni/Fe/Co oscillates with Fe film thickness. Because of the complex structure and magnetic ordering of fcc Fe,^{13–16} the interpretation of such an oscillation could be complicated by various factors, therefore it is interesting and critical to check whether it really reflects the intrinsic property of interlayer coupling on the magnetic anisotropy.

Here we present the work in a Ni/Cu/Co sandwich to study the effect of interlayer coupling on the magnetic anisotropy of Ni layer. There are some advantages for choosing the Ni/Cu/Co sandwich. On the one hand, the Ni/Cu/Co sandwich can be easily epitaxially grown on Cu(100) substrate with high sample quality,^{17,18} and the interlayer coupling as well as its effect on T_C has been well established.¹⁰ On the other hand, while the magnetization of Co layer is always in plane, the magnetization of Ni layer can be either in plane or out of plane depending on the thickness of Ni film. Simply by monitoring the signal in polar magneto-optic Kerr effect (MOKE), the out-of-plane magnetization of Ni layer can be separated from Co layer without using any chemically resolved techniques such as x-ray magnetic cir-

cular dichroism or PEEM. The well-known SRT of Ni on Cu(100) (Ref. 19) will be used as a fingerprint to investigate the oscillatory magnetic anisotropy caused by the interlayer coupling.

Experiments were performed in an ultrahigh vacuum system with a base pressure below 4×10^{-8} Pa, equipped with an evaporation system for molecular beam epitaxially growth, surface analysis facilities including low-energy electron diffraction (LEED), reflected high-energy electron diffraction (RHEED) and Auger electron spectrum (AES), and *in situ* MOKE setup. The Cu(100) substrate was prepared by cycles of 1 keV Ar⁺ bombardment at 300 K, followed by annealing at 873 K for 15 min. This cleaning procedure was repeated until a sharp (1×1) LEED pattern was observed and no contamination can be detected by AES.¹⁵ All depositions were performed at room temperature (300 K).

A representative sample of 8 monolayer (ML) Ni/5 ML Cu/5 ML Co is characterized by LEED and RHEED. As shown in Fig. 1(a), a nice (1×1) pattern is observed by LEED, taken with an incident electron-beam energy of 70 eV. The RHEED pattern, taken with the incident electron

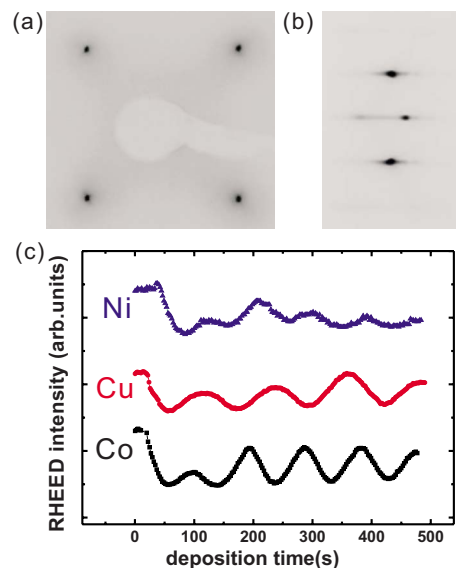


FIG. 1. (Color online) (a) LEED (taken at 70 eV) and (b) RHEED patterns of the representative 8ML Ni/5ML Cu/5ML Co/Cu(100) sample. (c) RHEED oscillations for Co, Cu, and Ni layers as a function of deposition time. Clear oscillations indicate the well-defined layer-by-layer growth mode.

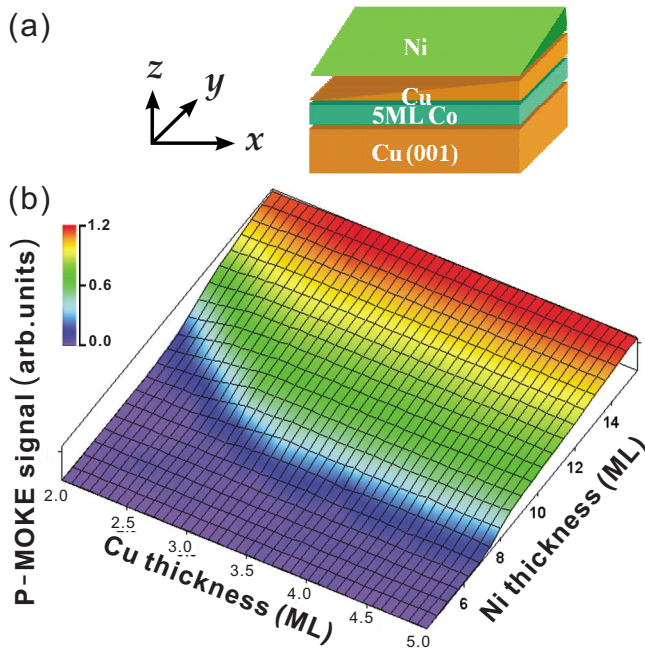


FIG. 2. (Color online) (a) Schematic structure of the double-wedge sample in which the Cu and Ni thicknesses vary along x and y directions independently. (b) P-MOKE signals as a function of Cu and Ni layers thicknesses.

beam along the substrate $[110]$ direction, is shown in Fig. 1(b). Intensities of (10) spots in the RHEED patterns were recorded as a function of time during the depositions of Co, Cu, and Ni layers, respectively, and shown in Fig. 1(c), clear oscillations can be seen for each layer, reflecting a well-defined layer-by-layer growth mode. Deposition rates were calculated from the oscillation periods so that all thicknesses can be precisely calibrated to minimize the uncertainty.

Double-wedge samples were used as illustrated in Fig. 2(a). The Cu and Ni wedges were deposited on 5 ML Co on Cu(100) along the x and y directions, respectively. By scanning with the laser spot of MOKE over the sample, we can find any desired combination of different thicknesses of Cu and Ni layers. Polar MOKE (P-MOKE) signal, which is sensitive to the out-of-plane magnetization of Ni layer, was measured as a function of Cu and Ni thicknesses at room temperature and plotted in Fig. 2(b). In the whole range of Cu thickness, the SRT of Ni can be observed. Two distinct regions of Cu thickness can be separated by the behavior of SRT. (i) For $d_{\text{Cu}} < 3$ ML, there should be strong ferromagnetic coupling between Co and Ni layers in this very thin region, which strongly favors aligning the magnetization of Ni in plane and thus increases the d_c of Ni as shown in Fig. 2(b). (ii) For $d_{\text{Cu}} > 3$ ML, unlike the Ni/Fe/Co case,¹¹ the d_c is around 8 ML and seems not sensitive to the Cu spacer layer thickness from the first glance.

However if we focus on the Ni layer of 8 ML, where the SRT happens, the results look very different. As shown by red dots in Fig. 3, clear oscillation in the P-MOKE signal can be observed as a function of Cu layer thickness. For the peaks of oscillation at 3.6 and 4.8 ML, the magnetization is out of plane; while for valleys at 4.2 and 5.4 ML, it is in plane. This oscillation indicates that the easy axis of the Ni

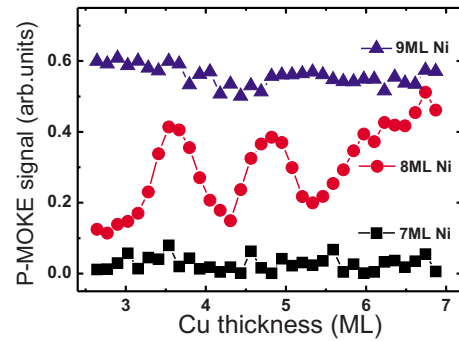


FIG. 3. (Color online) P-MOKE signal of Ni/Cu wedge/5 ML Co as a function of Cu spacer layer thickness with a Ni layer of 7 ML (black squares), 8 ML (red dots), and 9 ML (blue triangles), respectively. The signal for 8 ML (d_c of SRT) has oscillation.

layer changes between in plane and out of plane, reflecting an oscillatory magnetic anisotropy as a function of Cu thickness. The P-MOKE data for 7 ML (black squares) and 9 ML (blue triangles) Ni are also plotted for comparison. In both cases no oscillation can be distinguished. For 7 ML Ni, because the magnetization is in plane before the SRT, the near zero P-MOKE signal was observed; for 9 ML Ni, the SRT has finished and the magnetization is out of plane, thus a near constant signal was observed.

In order to establish the relation between the oscillatory magnetic anisotropy and interlayer coupling, we need to directly compare them within the same sample. So we covered the sample with 2 ML Co, which coupling directly with the 8 ML Ni and pushing the magnetization of Ni in plane. Then the types of interlayer coupling were determined from the longitudinal MOKE (L-MOKE) measurements as described in the following. Typical hysteresis loops for ferromagnetic and antiferromagnetic interlayer coupling are shown in Figs. 4(a) and 4(b), respectively. For ferromagnetic coupling (FC), square loops with 100% remanent magnetization can be observed because the magnetizations are coupled to the same direction and behave like one layer. While for antiferromagnetic coupling (AFC), loops are quite different with a plateau appeared in low field, caused by the overall cancellation of magnetizations in the sandwich. The nonzero signal in the plateau is due to the unequal magnetization on two sides of the Cu spacer. As the magnetic field increased, the AFC is overcome and the magnetizations are forced to align along the external field, resulting in a high and flat saturate magnetization again. For AFC and FC, the remanent magnetization will be a minimum or maximum, respectively. We can use the remanent magnetization signal as an approximate measure of the coupling type. The remanent L-MOKE signal is shown by black squares in Fig. 4(c), the AFC and FC are marked at their corresponding thicknesses, respectively. The positions for no coupling (NC), which should be in between of AFC and FC, are marked by red arrows as well.

For comparison the P-MOKE signal for 8 ML Ni taken from Fig. 3 is also plotted in Fig. 4(c) (red dots). For both FC (3.1 and 5.4 ML) and AFC (4.2 ML), the P-MOKE signal is a minimum, indicating an in-plane magnetization; while for NC (3.6 and 4.8 ML), the signal is a maximum, indicating an out-of-plane magnetization. The FC or AFC favor the mag-

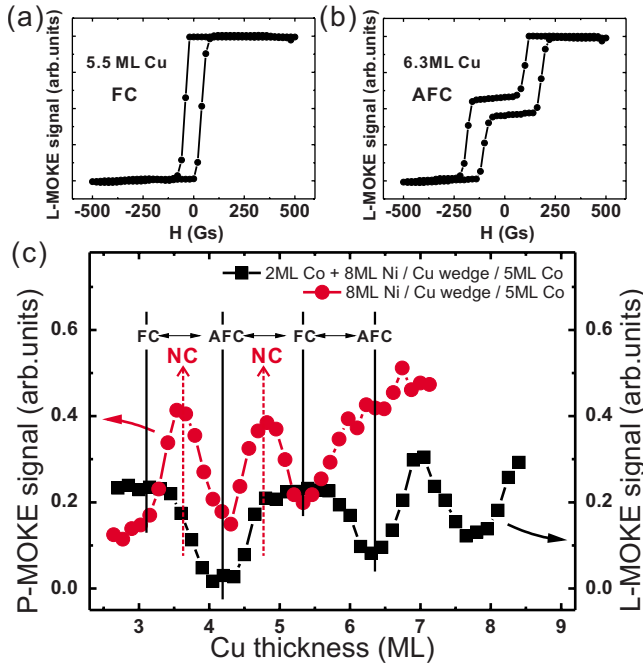


FIG. 4. (Color online) L-MOKE hysteresis loops for 2 ML Co/8 ML Ni/Cu wedge/5 ML Co with (a) $d_{\text{Cu}}=5.5$ and (b) 6.3 ML, in which ferromagnetic and antiferromagnetic interlayer coupling can be seen, respectively. (c) Remanent signal (black squares) taken from L-MOKE loops and P-MOKE signal (red dots) taken from Fig. 3 are plotted together as a function of Cu thickness. The types of coupling are marked according to the L-MOKE signal, and has good agreement with P-MOKE signal oscillation.

netization of Ni layer parallel or antiparallel to the magnetization of Co layer, which is in plane. So no matter FC or AFC, the interlayer coupling will always contribute an in-plane magnetic anisotropy, which yields a minimum of P-MOKE signal. For NC, the strength of coupling is around zero and its effect is negligible, thus a maximum of P-MOKE signal should be observed. The good agreement between the P-MOKE signal oscillation and the interlayer coupling confirms that the oscillatory magnetic anisotropy of Ni layer is attributed to the oscillatory interlayer coupling. The disappearance of P-MOKE signal oscillation as $d_{\text{Cu}} > 6$ ML, is presumably caused by the decay of the interlayer coupling strength,²⁰ as well as the interface roughness which can affect both the interlayer coupling²¹ and magnetic anisotropy.²²

It is worth noting that magnetic anisotropy can also be affected by the hybridization between the pronounced quantum-well states in Cu layer²³ and d bands of the magnetic layer, as reported by Weber *et al.*²⁴ in a Cu/Co/Cu(100) system; however, the oscillation is not a simple periodic but a more complicated one as discussed in details there. The oscillatory behavior observed here can be explained by the effective total magnetic anisotropy energy density for Ni

film. Following Baberschke and Farle's discussion,^{19,25} it can be written as

$$E = -\bar{K}_2 \cos^2 \theta - \frac{1}{8} K_{4\parallel} (3 + \cos 4\varphi) \sin^4 \theta - K_c \sin \theta \cos \varphi, \quad (1)$$

where $\bar{K}_2 = K_2 - \frac{1}{2} \mu_0 M^2$ is the effective second-order anisotropy constant, including magnetocrystalline and dipolar effects, $K_{4\parallel}$ are the fourth-order anisotropy constant, θ and φ are angles with respect to the surface normal and [001]. The interlayer coupling acts as an in-plane magnetic field for Ni,²⁶ whose direction depends on the magnetization of Co. This serves as an unidirectional anisotropy in the total energy as described as the last term in Eq. (1). The anisotropy constant K_c satisfies $K_c d_{\text{Ni}} = J M_{\text{Ni}} M_{\text{Co}}$.

In general, K_2 dominates over all the other terms in Eq. (1). This explains why the magnetization is in plane for the 7 ML Ni layer, as $K_2 < 0$, and perpendicular for the 9 ML layer, as $K_2 > 0$.¹⁹ For the 8 ML Ni layer, where the SRT occurs, K_2 is close to zero due to the cancellation of volume and interface/surface contributions.¹⁹ Now the effect of interlayer coupling K_c can compete with the sum for K_2 and $K_{4\parallel}$ terms. For the case of FC ($J > 0$) or AFC ($J < 0$), K_c overcomes the other two terms and favors an in-plane ($\theta = 90^\circ$) magnetization which is parallel ($\varphi = 0^\circ$) or antiparallel ($\varphi = 180^\circ$) to the Co magnetization. This leads to minimum of P-MOKE signals observed. For the case of NC ($J = 0$), K_c is zero. The perpendicular magnetic anisotropy of Ni layer in this case is mainly due to the uncompensated part of K_2 , which is still larger than $K_{4\parallel}$. The biquadratic interlayer coupling, which favors the perpendicular magnetic alignment of the Ni magnetization, could also contribute to the perpendicular magnetic anisotropy,²⁷ which would explain the maximum in the P-MOKE signals observed.

In conclusion, the magnetic anisotropy and interlayer coupling of epitaxially grown Ni/Cu/Co sandwich on Cu(100) has been studied *in situ* as a function of Cu and Ni thicknesses by MOKE. An oscillatory magnetic anisotropy, varying between in plane and out of plane as a function of Cu thickness, was observed for 8 ML Ni, where the SRT happens exactly. By comparing the magnetic anisotropy and interlayer coupling within the same sample, we clearly establish that the oscillatory magnetic anisotropy is attributed to the interlayer coupling between Ni and Co layers. This tuning effect of magnetic anisotropy, which can be precisely controlled through space layer thickness, would be helpful for tailoring of magnetic materials in future applications.

This work was supported by MSTC (Grants No. 2006CB921303 and No. 2009CB929203), NSFC (Grants No. 10834001 and No. 10621063), and the Shanghai Committee of Science and Technology, China (Grant No. 09JC1401000).

*xfjin@fudan.edu.cn

- ¹S. S. Parkin *et al.*, *J. Appl. Phys.* **85**, 5828 (1999).
- ²W. J. Gallagher and S. S. Parkin, *IBM J. Res. Dev.* **50**, 5 (2006).
- ³A. Ney, G. Pampuch, R. Koch, and K. H. Ploog, *Nature (London)* **425**, 485 (2003).
- ⁴C. S. Tian and X. F. Jin *et al.*, *Phys. Rev. Lett.* **94**, 137210 (2005).
- ⁵J. Wenisch, C. Gould, L. Ebel, J. Storz, K. Pappert, M. J. Schmidt, C. Kumpf, G. Schmidt, K. Brunner, and L. W. Molenkamp, *Phys. Rev. Lett.* **99**, 077201 (2007).
- ⁶K. Baberschke, *Appl. Phys. A: Mater. Sci. Process.* **62**, 417 (1996).
- ⁷W. Weber, D. A. Wesner, G. Güntherodt, and U. Linke, *Phys. Rev. Lett.* **66**, 942 (1991).
- ⁸J. Hong, R. Q. Wu, J. Lindner, E. Kosubek, and K. Baberschke, *Phys. Rev. Lett.* **92**, 147202 (2004).
- ⁹W. Guo and D. L. Lin, *Phys. Rev. B* **67**, 224402 (2003).
- ¹⁰A. Ney, F. Wilhelm, M. Farle, P. Pouloupoulos, P. Srivastava, and K. Baberschke, *Phys. Rev. B* **59**, R3938 (1999).
- ¹¹C. Won, Y. Z. Wu, H. W. Zhao, A. Scholl, A. Doran, and Z. Q. Qiu, *Phys. Rev. B* **68**, 052404 (2003).
- ¹²H. J. Choi, W. L. Ling, A. Scholl, J. H. Wolfe, U. Bovensiepen, F. Toyama, and Z. Q. Qiu, *Phys. Rev. B* **66**, 014409 (2002).
- ¹³J. Thomassen, F. May, B. Feldmann, M. Wuttig, and H. Ibach, *Phys. Rev. Lett.* **69**, 3831 (1992).
- ¹⁴Dongqi Li, M. Freitag, J. Pearson, Z. Q. Qiu, and S. D. Bader, *Phys. Rev. Lett.* **72**, 3112 (1994).
- ¹⁵D. Qian, X. F. Jin, J. Barthel, M. Klaua, and J. Kirschner, *Phys. Rev. Lett.* **87**, 227204 (2001).
- ¹⁶M. Zharnikov, A. Dittschar, W. Kuch, C. M. Schneider, and J. Kirschner, *Phys. Rev. Lett.* **76**, 4620 (1996).
- ¹⁷W. Kuch, J. Gilles, Xingyu Gao, and J. Kirschner, *J. Magn. Magn. Mater.* **242-245**, 1246 (2002).
- ¹⁸W. Kuch, L. I. Chelaru, K. Fukumoto, F. Porrati, F. Offi, M. Kotsugi, and J. Kirschner, *Phys. Rev. B* **67**, 214403 (2003).
- ¹⁹B. Schulz and K. Baberschke, *Phys. Rev. B* **50**, 13467 (1994).
- ²⁰R. K. Kawakami, E. Rotenberg, E. J. Escorcia-Aparicio, H. J. Choi, J. H. Wolfe, N. V. Smith, and Z. Q. Qiu, *Phys. Rev. Lett.* **82**, 4098 (1999).
- ²¹E. Holmström, L. Nordström, L. Bergqvist, B. Skubic, B. Hjörvarsson, I. A. Abrikosov, P. Svedlindh, and O. Eriksson, *Proc. Natl. Acad. Sci. U.S.A.*, **101**, 4742 (2004).
- ²²F. Matsui, T. Matsushita, Y. Kato, M. Hashimoto, K. Inaji, F. Z. Guo, and H. Daimon, *Phys. Rev. Lett.* **100**, 207201 (2008).
- ²³J. E. Ortega, F. J. Himpsel, G. J. Mankey, and R. F. Willis, *Phys. Rev. B* **47**, 1540 (1993).
- ²⁴W. Weber, A. Bischof, R. Allenspach, Ch. Würsch, C. H. Back, and D. Pescia, *Phys. Rev. Lett.* **76**, 3424 (1996).
- ²⁵C. Klein, R. Ramchal, A. K. Schmid, and M. Farle, *Phys. Rev. B* **75**, 193405 (2007).
- ²⁶Y. Z. Wu, C. Won, A. Scholl, A. Doran, H. W. Zhao, X. F. Jin, and Z. Q. Qiu, *Phys. Rev. Lett.* **93**, 117205 (2004).
- ²⁷M. Rührig, R. Schäfer, A. Hubert, R. Mosler, J. A. Wolf, S. Demokritov, and P. Grünberg, *Phys. Status Solidi A* **125**, 635 (1991); J. C. Slonczewski, *Phys. Rev. Lett.* **67**, 3172 (1991).